Revista Colombiana de Estadística - Applied Statistics
January 2021, volume 44, issue 1, pp. 23 a 41
http://dx.doi.org/10.15446/rce.v44n1.84779

On Some Statistical Properties of the Spatio-Temporal Product Density

Sobre algunas propiedades estadísticas de la densidad producto espacio-temporal

Felipe Rodríguez-Berrio[1,a], Francisco J. Rodríguez-Cortés[2,b], Jorge Mateu[3,c], Giada Adelfio[4,d]

[1]Ingeniería Ambiental, Facultad de Ingeniería, Universidad de Antioquia, Medellín, Colombia

[2]Escuela de Estadística, Facultad de Ciencias, Universidad Nacional de Colombia, Medellín, Colombia

[3]Departamento de Matemáticas, Escuela Superior de Tecnología y Ciencias Experimentales, Universitat Jaume I, Castellón, España

[4]Dipartimento di Scienze Economiche, Aziendali e Statistiche, Università degli Studi di Palermo, Palermo, Italy

Abstract

We present an extension of the non-parametric edge-corrected Ohser-type kernel estimator for the spatio-temporal product density function. We derive the mean and variance of the estimator and give a closed-form approximation for a spatio-temporal Poisson point process. Asymptotic properties of this second-order characteristic are derived, using an approach based on martingale theory. Taking advantage of the convergence to normality, confidence surfaces under the homogeneous Poisson process are built. A simulation study is presented to compare our approximation for the variance with Monte Carlo estimated values. Finally, we apply the resulting estimator and its properties to analyse the spatio-temporal distribution of the invasive meningococcal disease in the Rhineland Regional Council in Germany.

***Key words*:** Envelope; Invasive meningococcal disease; Lindeberg condition; Ohser-type estimator; Second-order product density.

[a]M.Sc. E-mail: felipe.rodriguez@udea.edu.co
[b]Ph.D. E-mail: frrodriguezc@unal.edu.co
[c]Ph.D. E-mail: mateu@uji.es
[d]Ph.D. E-mail: giada.adelfio@unipa.it

Resumen

En este artículo, presentamos un estimador para la función de densidad producto de un patrón de puntos en espacio-tiempo. Este estimador es una extensión del estimador no paramétrico de Ohser, el cuál está basado en una función Kernel y ponderado por un corrector de borde. Deducimos la media y la varianza del estimador y, a su vez, damos una aproximación analítica para el caso de un patrón Poisson (completamente aleatorio). Adicionalmente, estudiamos ciertas propiedades asintóticas de nuestro estimador utilizando un enfoque basado en la teoría de martingalas y construimos superficies de confianza para el caso de aleatoriedad completa. Presentamos un estudio de simulación para comparar nuestra aproximación de la varianza con los valores estimados a través del método Monte Carlo. Finalmente, utilizamos nuestro estimador para analizar la distribución espacio-temporal de los registros de una enfermedad meningocócica invasiva en la provincia del Rin en Alemania.

***Palabras clave*:** Condición de Lindeberg; Densidad de producto de segundo orden; Envoltura; Enfermedad meningocócica invasiva; Estimador de tipo Ohser.

1. Introduction

A large amount of point pattern data sets are collected in a wide range of scientific settings, such as environmental sciences, climate prediction and meteorology, epidemiology, image analysis, agriculture, and astronomy. While the statistical methodology for analysing point pattern data sets in time (Cox & Isham 1980, Daley & Vere-Jones 2003) and space (Diggle 2013, Møller & Waagepetersen 2004, Illian et al. 2008, Chiu et al. 2013) is rather well developed, today the focus is on spatio-temporal point processes (Diggle 2013, González et al. 2016), where each point represents the location and time of an event. Thus we have data of the form $(\mathbf{u}_i, s_i) \in W \times T \subset \mathbb{R}^2 \times \mathbb{R}$, $i = 1, \ldots, n$. We consider here processes that are temporally and spatially continuous on a sufficiently large support to justify formulating explicitly second-order spatio-temporal tools for the data.

Second-order functions play an essential role in the practical analysis of point patterns, regarding both exploratory and modelling strategies. Usually, the K-function and the pair correlation function are used for model checking (Møller & Ghorbani 2015), and parameter estimation (Møller & Ghorbani 2012). The second-order product density function (hereafter product density) is also useful for both exploratory and explanatory statistical analysis (Siino et al. 2018). The size and shape of these functions help to figure out the type of interaction within the point pattern data to further propose suitable point process models.

Gabriel & Diggle (2009) extended the inhomogeneous K-function (Baddeley et al. 2000) to the spatio-temporal setting for second-order intensity-reweighted stationary point processes. The spatio-temporal inhomogeneous K-function (STIK-function) or equivalently the spatio-temporal pair correlation function are thus utilised to analyse spatio-temporal correlations (Gabriel & Diggle 2009, Gabriel et al. 2010, 2013, Gabriel 2014). (Møller & Ghorbani 2012) studied the assumption of spatio-temporal separability of the STIK-function. These two

functions rely very much upon first-order characteristics which are unknown in practice, and replacing the intensity by an estimate must be made carefully as it may imply bias (Baddeley et al. 2000, Gabriel 2014). We note that for Poisson processes, the product density becomes the product of the first-order intensities. In the most general case, the product density is a non-standardised second-order characteristic which does not depend on the intensity function and provides, in a general sense, the same amount of information about the nature of the underlying process as other second-order descriptors (González et al. 2016).

In literature, several estimators have been proposed to estimate the product density function in a spatial setting, see for instance (Fiksel 1988, Ohser 1983, Stoyan et al. 1993). One of the most elegant estimators of the spatial product density, in terms of programming and mathematical calculation, is Ohser's estimator (Stoyan et al. 1993). In this paper, we extend the idea in Ohser (1983) to the spatio-temporal case to provide an estimation of the product density function. As the estimated second-order characteristics may deviate from their theoretical counterparts due to statistical fluctuations, it is highly important to be able to build confidence surfaces for the theoretical functions. This can be done assuming normality under the Poisson process (see Section 5). These surfaces can also be used for model checking and to further discriminate between clustering or regularity behaviour. Little attention has been paid so far to study the first- and second-order moments (mean and variance) of the second-order characteristics of spatio-temporal point processes. In the spatial context, we refer to (Ripley 1988) who gave the variance for some estimators of the spatial K-function for homogeneous Poisson and Binomial point patterns. Later, (Stoyan et al. 1993) approximated the variance of the spatial product density and the spatial pair correlation functions, and Cressie & Collins (2001a) obtained closed form expressions for the mean and variance of the local spatial product densities. Guan (2009) developed a non-parametric estimator for the K-function variance under inhomogeneity for a parametric intensity and under the assumption of SOIRS. To the best of our knowledge, nothing has been developed in the spatio-temporal context. González et al. (2020) extend to the spatio-temporal context the hypothesis test to prove that two (or more) observed point patterns with replications are realisations of point processes that have the same second-order descriptors. Here, we follow the original idea in (Stoyan et al. 1993) to extend it to the spatio-temporal case and obtain exact and approximate expressions of the mean and variance of the proposed estimator.

The rest of the paper is organised as follows. In Section 2, we recall some theoretical background of first- and second-order characteristics of spatio-temporal point processes. In Section 3 we propose a non-parametric estimator for the product density and obtain its mean and variance for the general case and for homogeneous Poisson processes. Also, we include some asymptotic results for the spatio-temporal product density. We then present some simulation results in Section 5. We describe an application of our methodology to spatio-temporal data on the invasive meningococcal disease in the Rhineland Regional Council in Germany between 2003 and 2007 in Section 6. We end the paper with some final conclusions.

2. Definitions and Statistical Background

We consider a finite realisation $\mathbf{x} = \{(\mathbf{u}_1, s_1), \ldots, (\mathbf{u}_n, s_n)\}$ of a spatio-temporal point process X within a bounded spatio-temporal region $W \times T \subset \mathbb{R}^2 \times \mathbb{R}$, where a point $(\mathbf{u}, s) \in X$ denotes an event at $\mathbf{u} \in \mathbb{R}^2$ occurring at time $s \in \mathbb{R}$. We consider a spatio-temporal point process without any overlapping points as a random countable subset X of $\mathbb{R}^2 \times \mathbb{R}$. Let $N(C)$ denote the number of events falling in an arbitrary bounded region $C \subset \mathbb{R}^2 \times \mathbb{R}$, $\Theta_h = \{(\mathbf{u}_1, s_1), \ldots, (\mathbf{u}_h, s_h) \in X\}$ is a set of h-tuples of events in X, $\int_{C^{\otimes h}} = \int_C \ldots \int_C$ for h times and $C = W \times T$.

Assume that X has a spatio-temporal hth-order product density $\rho^{(h)}$, for $h = 1, 2, \ldots$. Then for any non-negative measurable function f defined on $(\mathbb{R}^2 \times \mathbb{R})^{\otimes h}$,

$$\mathbb{E} \sum_{\Theta_h}^{\neq} f((\mathbf{u}_1, s_1), \ldots, (\mathbf{u}_h, s_h)) = \int_{(\mathbb{R}^2 \times \mathbb{R})^{\otimes h}} f((\mathbf{u}_1, s_1), \ldots, (\mathbf{u}_h, s_h)) \times \rho^{(h)}((\mathbf{u}_1, s_1), \ldots, (\mathbf{u}_h, s_h)) \prod_{i=1}^{h} \mathrm{d}(\mathbf{u}_i, s_i), \tag{1}$$

where $\sum^{\neq}$ means that we sum over h pairwise distinct points. Considering (1), in particular for $h = 1$ and $h = 2$, the hth-order product density functions are called the intensity function and product density, respectively. A process for which $\rho^{(1)}(\mathbf{u}, s) = \rho$ for all $(\mathbf{u}, s)$ is called homogeneous or first-order stationary and ρ is called intensity. Throughout this paper, we assume that the point process X is second-order intensity-reweighted stationary (SOIRS), i.e.

$$\rho^{(2)}((\mathbf{u}, s), (\mathbf{v}, \ell)) = \rho(\mathbf{u}, s)\rho(\mathbf{v}, \ell) g(\mathbf{u} - \mathbf{v}, s - \ell), \qquad (\mathbf{u}, s), (\mathbf{v}, \ell) \in \mathbb{R}^2 \times \mathbb{R},$$

where the pair correlation function g depends only on the spatial difference $\mathbf{u} - \mathbf{v}$ and time lag $s - \ell$ (Gabriel & Diggle 2009). Further, if for any spatial rotation around the origin, the rotated point process has the same distribution as the original process then $g(\mathbf{u} - \mathbf{v}, s - \ell) = g_0(\|\mathbf{u} - \mathbf{v}\|, |s - \ell|)$ for some non-negative function g_0, where $\|\cdot\|$ denotes the Euclidean norm in $\mathbb{R}^2$ and $|\cdot|$ denotes the absolute value in $\mathbb{R}$ we then say that the process is isotropic; for more details see González et al. (2020). Throughout the paper, we assume that the process is isotropic.

3. Product Density Estimation

We extend the idea developed by Ohser (1983) to estimate the product density function. A spatio-temporal kernel density estimator of $\rho^{(2)}(r, t)$ takes the basic form of a smoothed three-dimensional histogram,

$$(|W||T|)^{-1} \sum_{(\mathbf{u},s),(\mathbf{v},l) \in \mathbf{x}}^{\neq} \kappa_{\epsilon,\delta}(\|\mathbf{u} - \mathbf{v}\| - r, |s - \ell| - t),$$

where $|W|$ and $|T|$ denote the area of W and the length of T, respectively, and $\kappa_{\epsilon,\delta}(\cdot,\cdot)$ stands for a kernel function. For the sake of simplicity, we consider the multiplicative form $\kappa_{\epsilon,\delta}(\|\mathbf{u}-\mathbf{v}\|-r,|s-\ell|-t) = \kappa_{1\epsilon}(\|\mathbf{u}-\mathbf{v}\|-r)\,\kappa_{2\delta}(|s-\ell|-t)$, where $\kappa_{1\epsilon}$ and $\kappa_{2\delta}$ are one-dimensional kernel functions with bandwidths ϵ and δ, respectively. An edge-corrected kernel estimator of the product density function is given by

$$\widehat{\rho^{(2)}}_{\epsilon,\delta}(r,t) = \sum_{(\mathbf{u},s),(\mathbf{v},l)\in\mathbf{x}}^{\neq} \frac{\kappa_{1\epsilon}(\|\mathbf{u}-\mathbf{v}\|-r)\,\kappa_{2\delta}(|s-\ell|-t)}{c(r,t)}, \tag{2}$$

where $r > \epsilon > 0$, $t > \delta > 0$ and $c(r,t) = 4\pi r\gamma_W(r)\gamma_T(t)$. Here $\gamma_W(r)$ and $\gamma_T(t)$ are the spatial and temporal set covariance functions, respectively. The set covariance function of a sampling window W is defined as the volume of the intersection $W \cap W_{-\omega}$ where $W_{-\omega}$ is the set shifted by the vector $-\omega$ (see more details in Chiu et al. 2013). For small r, $\gamma_W(r)$ can generally be approximated by $\gamma_W(r) \approx |W| - \frac{U(W)}{\pi}r$, where $U(W)$ is the perimeter of W (Stoyan et al. 1993). For a small t it follows that $\gamma_T(t) = |T| - t$.

3.1. Mean and Variance of the Estimator

We now obtain the mean and variance of the product density estimator (2) for the general case. We assume that the product density function is continuous. Using (1) with $h = 2$, the estimator (2) satisfies

$$\begin{aligned}\mathbb{E}\left[\widehat{\rho^{(2)}}_{\epsilon,\delta}(r,t)\right] &= \int_{(\mathbb{R}^2\times\mathbb{R})^{\otimes 2}} \frac{\kappa_{1\epsilon}(\|\mathbf{x}-\mathbf{y}\|-r)\kappa_{2\delta}(|\xi-\eta|-t)}{4\pi\gamma_W(r)\gamma_T(t)r} \\ &\qquad \times \rho^{(2)}(\|\mathbf{x}-\mathbf{y}\|,|\xi-\eta|)\mathrm{d}(\mathbf{x},\xi)\mathrm{d}(\mathbf{y},\eta) \\ &= \int_{-r/\epsilon}^{\infty}\int_{-t/\delta}^{\infty} \frac{\kappa_1(u)\kappa_2(v)\gamma_W(r+\epsilon u)\gamma_T(t+\delta v)}{r\gamma_W(r)\gamma_T(t)} \\ &\qquad \times \rho^{(2)}(r+\epsilon u, t+\delta v)(r+\epsilon u)\mathrm{d}u\,\mathrm{d}v. \end{aligned} \tag{3}$$

If (r,t) is a continuity point of $\rho^{(2)}(r,t)$, then

$$\lim_{(\epsilon,\delta)\to(0,0)} \mathbb{E}\left[\widehat{\rho^{(2)}}_{\epsilon,\delta}(r,t)\right] = \rho^{(2)}(r,t),$$

hence, $\widehat{\rho^{(2)}}_{\epsilon,\delta}(r,t)$ is an asymptotic unbiased estimator for the spatio-temporal product density.

To calculate the variance, under the intensity reweighted stationarity assumption, application of Campbell's formula (Illian et al. 2008, Chiu et al. 2013) for the spatio-temporal case implies that

$$\mathbb{E}\left[\left(\widehat{\rho^{(2)}}_{\epsilon,\delta}(r,t)\right)^2\right] = \frac{1}{(c(r,t))^2}\left[4E_1(C) + 2E_2(C) + E_3(C)\right] \tag{4}$$

where

$$E_1(C) = \int_{C^{\otimes 3}} \kappa_{1\epsilon}(\|\mathbf{x}-\mathbf{y}\|-r)\kappa_{1\epsilon}(\|\mathbf{x}-\mathbf{z}\|-r)\kappa_{2\delta}(|\xi-\eta|-t)\kappa_{2\delta}(|\xi-\zeta|-t) \times \rho^{(3)}((\|\mathbf{x}-\mathbf{y}\|,|\xi-\eta|),(\|\mathbf{x}-\mathbf{z}\|,|\xi-\zeta|))\mathrm{d}(\mathbf{x},\xi)\mathrm{d}(\mathbf{y},\eta)\mathrm{d}(\mathbf{z},\zeta),$$

$$E_2(C) = \int_{C^{\otimes 2}} \kappa_{1\epsilon}^2(\|\mathbf{x}-\mathbf{y}\|-r)\kappa_{2\delta}^2(|\xi-\eta|-t) \times \rho^{(2)}(\|\mathbf{x}-\mathbf{y}\|,|\xi-\eta|)\mathrm{d}(\mathbf{x},\xi)\mathrm{d}(\mathbf{y},\eta),$$

$$E_3(C) = \int_{C^{\otimes 4}} \kappa_{1\epsilon}(\|\mathbf{x}-\mathbf{y}\|-r)\kappa_{1\epsilon}(\|\mathbf{z}-\mathbf{w}\|-r)\kappa_{2\delta}(|\xi-\eta|-t)\kappa_{2\delta}(|\zeta-\gamma|-t) \times \rho^{(4)}((\|\mathbf{x}-\mathbf{y}\|,|\xi-\eta|),(\|\mathbf{x}-\mathbf{z}\|,|\xi-\zeta|),(\|\mathbf{x}-\mathbf{w}\|,|\xi-\eta|)) \times \mathrm{d}(\mathbf{x},\xi)\mathrm{d}(\mathbf{y},\eta)\mathrm{d}(\mathbf{z},\zeta)\mathrm{d}(\mathbf{w},\gamma). \quad (5)$$

Thus, to find an expression for the variance in terms of (ϵ,δ), we have to know the third- and fourth-order product densities, which opens new mathematical difficulties (see Guan 2009 for the spatial case).

3.2. Mean and Variance of the Product Density Estimator for a Homogeneous Poisson Process

For a homogeneous Poisson process with intensity ρ, when $(\epsilon,\delta)\to(0,0)$,

$$\mathbb{E}\left[\widehat{\rho^{(2)}}_{\epsilon,\delta}(r,t)\right] = \rho^2 \text{ and } \mathbb{V}\mathrm{ar}\left[\widehat{\rho^{(2)}}_{\epsilon,\delta}(r,t)\right] = \frac{1}{(c(r,t))^2}\left[4\rho^3 S_1 + 2\rho^2 S_2\right], \quad (6)$$

where S_1 and S_2 are given by

$$S_1 = \int_{C^{\otimes 3}} \kappa_{1\epsilon}(\|\mathbf{x}-\mathbf{y}\|-r)\kappa_{1\epsilon}(\|\mathbf{x}-\mathbf{z}\|-r) \times \kappa_{2\delta}(|\xi-\eta|-t)\kappa_{2\delta}(|\xi-\zeta|-t)\mathrm{d}(\mathbf{x},\xi)\mathrm{d}(\mathbf{y},\eta)\mathrm{d}(\mathbf{z},\zeta) = \int_C \left\{\int_C \kappa_{1\epsilon}(\|\mathbf{x}-\mathbf{y}\|-r)\kappa_{2\delta}(|\xi-\eta|-t)\,\mathrm{d}(\mathbf{y},\eta)\right\}^2 \mathrm{d}(\mathbf{x},\xi) = S_1^s S_1^t$$

and

$$S_2 = \int_{C^{\otimes 2}} \kappa_{1\epsilon}^2(\|\mathbf{x}-\mathbf{y}\|-r)\kappa_{2\delta}^2(|\xi-\eta|-t)\mathrm{d}(\mathbf{x},\xi)\mathrm{d}(\mathbf{y},\eta) = S_2^s S_2^t,$$

with

$$S_1^s = \int_W \left\{ \int_W \kappa_{1\epsilon}(\|\mathbf{x}-\mathbf{y}\|-r)\,\mathrm{d}\mathbf{y} \right\}^2 \mathrm{d}\mathbf{x}, \quad S_2^s = \int_{W^{\otimes 2}} \kappa_{1\epsilon}^2(\|\mathbf{x}-\mathbf{y}\|-r)\mathrm{d}\mathbf{x}\mathrm{d}\mathbf{y},$$
$$S_1^t = \int_T \left\{ \int_T \kappa_{2\delta}(|\xi-\eta|-t)\,\mathrm{d}\eta \right\}^2 \mathrm{d}\xi, \qquad S_2^t = \int_{T^{\otimes 2}} \kappa_{2\delta}^2(|\xi-\eta|-t)\mathrm{d}\xi\mathrm{d}\eta.$$

To show these two results, we note the following. For a homogeneous Poisson process with intensity ρ, the hth-order product density $\rho^{(h)}$ is equal to ρ^h, thus using (3) when $(\epsilon,\delta)\to(0,0)$,

$$\mathbb{E}\left[\widehat{\rho^{(2)}}_{\epsilon,\delta}(r,t)\right] = \int_{-r/\epsilon}^{\infty}\int_{-t/\delta}^{\infty} \frac{\kappa_1(u)\kappa_2(v)\gamma_W(r+u\epsilon)\gamma_T(t+\delta v)}{r\gamma_W(r)\gamma_T(t)} \times \rho^{(2)}(r+u\epsilon,t+\delta v)(r+u\epsilon)\mathrm{d}u\,\mathrm{d}v \to \rho^2.$$

To obtain the variance in (6), we should notice that $c(r,t)\widehat{\rho^{(2)}}_{\epsilon,\delta}(r,t)$ in (2) has the form

$$A = \sum_{(\mathbf{u},s),(\mathbf{v},l)\in\mathbf{x}}^{\neq} \kappa_{1\epsilon}\left(\|\mathbf{u}-\mathbf{v}\|-r\right)\kappa_{2\delta}\left(|s-\ell|-t\right).$$

So, using Campbell formula for the spatio-temporal case

$$\mathbb{E}\left[A\right] = \rho^2 \int_{C^{\otimes 2}} \kappa_{1\epsilon}(\|\mathbf{x}-\mathbf{y}\|-r)\kappa_{2\delta}(|\xi-\eta|-t)\,\mathrm{d}(\mathbf{x},\xi)\,\mathrm{d}(\mathbf{y},\eta)$$

and

$$\mathbb{E}\left[A^2\right] = 4\rho^3 S_1 + 2\rho^2 S_2 + \rho^4 S_3,$$

where S_1 and S_2 are given above, and S_3 is given by

$$S_3 = \int_{C^{\otimes 4}} \kappa_{1\epsilon}(\|\mathbf{x}-\mathbf{y}\|-r)\kappa_{1\epsilon}(\|\mathbf{z}-\mathbf{w}\|-r) \times \kappa_{2\delta}(|\xi-\eta|-t)\kappa_{2\delta}(|\zeta-\gamma|-t)\mathrm{d}(\mathbf{x},\xi)\mathrm{d}(\mathbf{y},\eta)\mathrm{d}(\mathbf{z},\zeta)\mathrm{d}(\mathbf{w},\gamma).$$

Further, $(\mathbb{E}[A])^2 = \rho^4 S_3$. Hence, $\mathbb{V}\mathrm{ar}[A] = 4\rho^3 S_1 + 2\rho^2 S_2$, and

$$\mathbb{V}\mathrm{ar}\left[\widehat{\rho^{(2)}}_{\epsilon,\delta}(r,t)\right] = \frac{1}{(c(r,t))^2}\left[4\rho^3 S_1 + 2\rho^2 S_2\right].$$

For the spatial case, and using the Epanechnikov kernel, (Stoyan et al. 1993) showed that $S_2^s = \frac{6}{5\epsilon}\left(|W|\pi r - U(W)\left(\frac{\epsilon^2}{7}+r^2\right)\right)$ and $S_1^s = 4\pi^2 r^2\big(|W|-D\big) +$

$4(r+\epsilon)^2(\pi-1)^2 D$, where $D = U(W)(r+\epsilon) - 4(r+\epsilon)^2$. For the temporal case, and using the uniform kernel, it is easy to show that

$$S_2^t = \frac{|T|}{\delta} \quad \text{and} \quad S_1^t = 4|T| - 8(t+\delta) + \frac{128}{3}t^2(t+\delta).$$

By combining the above expressions, an approximation of the variance of the product density estimator is obtained. In practice we substitute ρ in (6) by its estimator $\hat{\rho} = \frac{n}{|W||T|}$.

4. Martingale Characterisation of the Product Density

The convergence to normality is an important asymptotic property of the expectation of the product density function to build confidence surfaces under homogeneous Poisson processes. The central limit theorem for martingales is a straightforward result that, combining Theorems 4 and 6 in Adelfio & Schoenberg (2009), provides asymptotic convergence properties related to the normal distribution for a stochastic process. This classical result for the martingale difference process (Hall & Heyde 2014) can be enunciated in this context as follows.

Theorem 1 (Central limit theorem for martingales)**.** *If the martingale difference stochastic process* $\{Z_m, \mathcal{H}_m\}_{m=1}^{\infty}$*, with Borel* σ*-algebra* $\mathcal{H}_m = \sigma(Z_1, Z_2, \ldots, Z_m)$ *and* $\mathbb{E}[Z_j|\mathcal{H}_{j-1}] = 0$*, for* $j = 1, 2, \ldots$*, satisfies the following two conditions:*

1. *Lindeberg condition:* $\mathbb{E}[Z_j^2] < \infty$*,* $j = 1, 2, \ldots$ *such that for any* $\varepsilon > 0$*,*

$$\lim_{m\to\infty} \left(\frac{1}{s_m^2} \sum_{j=1}^{m} \mathbb{E}\left[Z_j^2 \, \mathbb{I}_{\{|Z_j| > \varepsilon s_m\}} \right] \right) = 0,$$

were $\mathbb{I}$ *is the indicator function and*

$$s_m^2 = \mathbb{V}ar\left[\sum_{j=1}^{m} Z_j \right] \to \infty \text{ as } m \to \infty.$$

2. $\mathbb{E}[\mathbb{E}[Z_j^2|\mathcal{H}_{j-1}]] = \mathbb{V}ar[Z_j]$*,* $j = 1, 2, \ldots$.

Then we have convergence in distribution to a standard normal random variable as $m \to \infty$*,*

$$\frac{1}{s_m} \sum_{j=1}^{m} Z_j \xrightarrow{d} N(0,1).$$

We do not prove these statements and concentrate on the characterisation of $\widehat{\rho^{(2)}}_{\epsilon,\delta}(r,t)$. Note that the Lindeberg condition is held if we set the process $Z_j = \widehat{\rho^{(2)}}_{\epsilon,\delta}(r,t) - \rho^{(2)}(r,t)$, with expectation zero and $\mathbb{V}\text{ar}[Z_j] = \mathbb{E}\left[\widehat{\rho^{(2)}}_{\epsilon,\delta}\right]^2$. Also, the third- and fourth-order product densities exist and are finite.

Theorem 2 (Martingale characterisation of $\widehat{\rho^{(2)}}_{\epsilon,\delta}(r,t)$)**.** *Let X be a simple spatio-temporal point process within a bounded spatio-temporal region $W \times T \subset \mathbb{R}^2 \times \mathbb{R}$ and with product density $\rho^{(2)}(r,t)$. The estimator defined in (2), with expectation given in the equation (3), is a martingale process, then*

$$\mathbb{E}\left[\widehat{\rho^{(2)}}_{\epsilon,\delta}(r,t) - \widehat{\rho^{(2)}}_{\epsilon,\delta}(r,t-1)|\widehat{\rho^{(2)}}(r,t-1)\right] = 0.$$

Proof. Given that $\widehat{\rho^{(2)}}_{\epsilon,\delta}(r,t-1)$ is measurable with respect to $\widehat{\rho^{(2)}}_{\epsilon,\delta}(r,t-1)$ then we have that

$$\begin{aligned}\mathbb{E}\left[\widehat{\rho^{(2)}}_{\epsilon,\delta}(r,t) - \widehat{\rho^{(2)}}_{\epsilon,\delta}(r,t-1)|\widehat{\rho^{(2)}}(r,t-1)\right] &= \mathbb{E}\left[\widehat{\rho^{(2)}}_{\epsilon,\delta}(r,t)|\widehat{\rho^{(2)}}(r,t-1)\right] \\ - \mathbb{E}\left[\widehat{\rho^{(2)}}_{\epsilon,\delta}(r,t-1)\right] &= \mathbb{E}\left[\widehat{\rho^{(2)}}_{\epsilon,\delta}(r,t)|\widehat{\rho^{(2)}}(r,t-1)\right] - \rho^{(2)}(r,t-1),\end{aligned}$$

since (r,t) is a continuity point of $\rho^{(2)}(r,t)$ then

$$\mathbb{E}\left[\widehat{\rho^{(2)}}_{\epsilon,\delta}(r,t)|\widehat{\rho^{(2)}}_{\epsilon,\delta}(r,t-1)\right] = \mathbb{E}\left[\widehat{\rho^{(2)}}_{\epsilon,\delta}(r,t-1)\right] = \rho^{(2)}(r,t-1),$$

then we have the result. Therefore, having defined a martingale starting from $\widehat{\rho^{(2)}}_{\epsilon,\delta}(r,t)$, its normality is proved if the conditions of Theorem 1 hold. □

Theorem 3. *Let X be a simple spatio-temporal point process in $\mathbb{R}^2 \times \mathbb{R}$ with product density function $\rho^{(2)}(r,t)$ such that $\mathbb{E}[\widehat{\rho^{(2)}}(r,t_j)|\mathcal{H}_j]$ for all t is bounded and there exists an $\alpha > 0$ such that $\mathbb{E}[\widehat{\rho^{(2+\alpha)}}(r,t_j)|\mathcal{H}_j]$ for all j is bounded. Moreover, let $Z_j = \widehat{\rho^{(2)}}(r,t_j) - \rho^{(2)}(r,t_j)$ be a process with expectation zero and $\mathbb{V}ar[Z_j] = \mathbb{E}\left[\widehat{\rho^{(2)}}_{\epsilon,\delta}(r,t_j)\right]^2$, with finite third- and fourth-order product densities. Finally, considering the temporal dimension, assume that for any j there exists $\tau_j = \sup\{\tau : N(\tau) = 1, N(\tau,\tau+r) = 0, \tau + r < t_j\}$, $r > 0$, that is there are not overlaps in time. Then*

$$\frac{1}{s_m}\sum_{j=1}^{m} Z_j \xrightarrow{d} N(0,1).$$

Proof. Starting from Theorem 2 and since $\mathbb{E}[Z_j] = \rho^{(2)}(r,t_j)$ and $\mathbb{E}[Z_j] < \infty$ for all j, and X is assumed to be simple, the Lindeberg condition is immediately proved. First note that

$$s_m^2 = \mathbb{V}\text{ar}\left[\sum_j^m Z_j\right] = \sum_j^m \mathbb{V}\text{ar}[Z_j] = \sum_j^m \mathbb{E}[Z_j^2].$$

Hence $\epsilon s_n \to \infty$ as $n \to \infty$. To prove condition 1 (Lindeberg condition) of Theorem 1, using the Hölder inequality, write

$$\sum_{j=1}^{m} \mathbb{E}\left[Z_j^2 \mathbb{I}_{\{|Z_j|>\varepsilon s_m\}}\right] \leq \sum_{j=1}^{m} \left(\mathbb{E}\left[|Z_j|^{2+\alpha}\right]\right)^{2/(\alpha+2)} \mathbb{P}\left[|Z_j| > \varepsilon\, s_m\right]^{\alpha/(\alpha+2)}$$
$$\leq \left(\sum_{j=1}^{m} \mathbb{E}\left[|Z_j|^{2+\alpha}\right]^{2/(\alpha+2)}\right) \left(\sum_{j=1}^{m} \mathbb{P}[|Z_j| > \varepsilon s_m]\right)^{\frac{\alpha}{(\alpha+2)}}.$$

Using Chebyshev inequality,

$$\sum_{j}^{m} \mathbb{P}[|Z_j| \geq \epsilon s_m] \leq \frac{\mathbb{E}[Z_j]^2}{\varepsilon^2 s_m^2} = \frac{1}{\varepsilon^2},$$

and $\mathbb{E}\left[Z_j^{2+\alpha}\right]$ remains bounded (from the assumption about $\mathbb{E}[\widehat{\rho^{(2+\alpha)}}(r,t)|\mathcal{H}_t]$), therefore $\sum_{j=1}^{m} \mathbb{E}\left[Z_j^2 \mathbb{I}_{\{|Z_j|>\varepsilon s_m\}}\right]$ grows less fast than s_m^2 and the Lindeberg condition holds.

Therefore, we have shown that

$$\frac{1}{s_m} Z \to N(0,1), \tag{7}$$

with $Z = \sum_{j=1}^{m} Z_j = \sum_{j=1}^{m} \left(\widehat{\rho^{(2)}}(r,t_j) - \rho^{(2)}(r,t_j)\right)$. □

A complete simulation exercise to check the normality property for the second-order characteristics is given in Adelfio et al. (2020). Therefore we take advantage of the computational results reported in this work which go in the same direction of the product density to omit presenting those results here.

5. Simulation Study

The spatio-temporal product density is a valuable tool for model fitting and checking in a spatio-temporal point process setting. The behaviour of the product density conveys useful information on the underlying structure of the pattern considering just the behaviour of the response surface over small values of spatial and temporal distances (r,t). For a Poisson process $\mathbb{E}[\widehat{\rho^{(2)}}_{\epsilon,\delta}(r,t)] \approxeq \rho^2$ which represents a plane and where $\widehat{\rho^{(2)}}_{\epsilon,\delta}(r,t)$ comes from (2). In general, for small values of (r,t), $\widehat{\rho^{(2)}}_{\epsilon,\delta}(r,t) > \rho^2$ indicates clustering and $\widehat{\rho^{(2)}}_{\epsilon,\delta}(r,t) < \rho^2$ indicates regularity or repulsion. To study the behaviour of the estimator for the product density, we conduct a simulation experiment under the assumption of complete spatio-temporal randomness. In addition, as we have developed a closed form expression for the variance in the Poisson case and based on the asymptotic

normality of the product density, we generate the corresponding confidence surfaces.

We set $W \times T = [0, 10]^2 \times [0, 10]$ and simulate spatio-temporal point patterns with a varying expected number of points $\mathbb{E}[N(C)] = 100, 200, 300$. We consider 100 repetitions per pattern and scenario, and use the R package stpp (Gabriel et al. 2013). We consider the spatial and temporal distances r and t spanning the sequence starting from $r > \epsilon > 0$ to 2.50 and $t > \delta > 0$ to 2.50 with small increments. Currently, there are different methods for bandwidth selection in the literature of spatial point processes. Minimisation of the mean integrated square error (MISE) (Berman & Diggle 1989), least square cross-validation (Guan 2007*b*), and composite likelihood cross-validation (Guan 2007*a*) are widely used techniques that have been developed in the literature. For example, in the spatial case, Fiksel (1988) suggested the use of the Epanechnikov kernel with bandwidth $\epsilon = 0.1\sqrt{5/\rho}$. In this paper, the dpik function of the R package Kernsmooth (Wand et al. 2019), (see Deng & Wickham 2011), is used for selecting bandwidth ϵ. Briefly, the dpik function chooses the bandwidth by the plug-in approach; see more details in Sheather & Jones (1991), and Wand & Jones (1994). For the temporal case, the uniform kernel is used, where we again calculate the bandwidth δ using the dpik function based on the time lag between the temporal instants of the process.

TABLE 1: Descriptive measures for the Monte Carlo mean estimates of the product density under homogeneous Poisson processes.

n	ϵ	δ	$\widehat{\rho^2}$	r	t	$Q_{5\%}(\widehat{\rho^{(2)}}_{\epsilon,\delta})$	$\widehat{\rho^{(2)}}_{\epsilon,\delta}$	$Q_{95\%}(\widehat{\rho^{(2)}}_{\epsilon,\delta})$	$\sigma(\widehat{\rho^{(2)}}_{\epsilon,\delta})$	$\widehat{\sigma}(\widehat{\rho^{(2)}}_{\epsilon,\delta})$
				1.132	0.541	0.009	0.010	0.014	0.003	0.003
				1.487	1.049	0.010	0.010	0.014	0.005	0.003
100	0.998	0.384	0.010	1.791	1.484	0.010	0.010	0.013	0.007	0.007
				2.145	1.992	0.010	0.010	0.014	0.011	0.013
				2.449	2.427	0.010	0.010	0.014	0.016	0.013
				1.132	0.541	0.039	0.040	0.052	0.009	0.010
				1.487	1.049	0.040	0.039	0.051	0.012	0.017
200	0.735	0.248	0.040	1.791	1.484	0.039	0.040	0.051	0.018	0.017
				2.145	1.992	0.039	0.039	0.050	0.029	0.027
				2.449	2.427	0.040	0.040	0.053	0.041	0.037
				1.132	0.541	0.087	0.090	0.108	0.015	0.013
				1.487	1.049	0.089	0.089	0.109	0.022	0.020
300	0.615	0.188	0.090	1.791	1.484	0.090	0.090	0.111	0.032	0.013
				2.145	1.992	0.090	0.091	0.110	0.051	0.042
				2.449	2.427	0.090	0.092	0.116	0.072	0.083

Table 1 shows some descriptive measures of the product density estimator for homogeneous Poisson point patterns generated by using the rpp function in stpp package. The spatial and the temporal bandwidths are estimated for each of the repetitions. The table displays the average optimal bandwidth for each sample size. We also studied the behaviour of the product density estimator with non-optimal bandwidths (the results are omitted here). The estimator in (2) proved to be robust showing small variations against a range of values for the bandwidths. From all possible grid cells, we have only shown the descriptive measures for some particular values of (r, t), for comparison purposes. These (r, t) values have been selected to cover the ranges of the spatial and temporal distances.

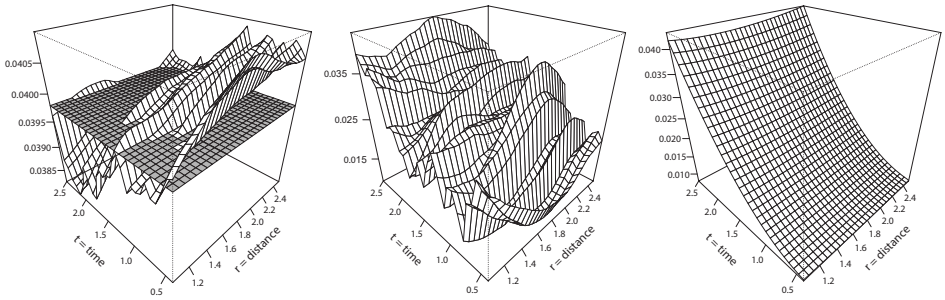

(a) Theoretical and estimated surfaces. (b) Average standard deviation surface. (c) Theoretical standard deviation surface.

FIGURE 1: Monte Carlo mean estimates of the product density functions and their standard deviation based on 100 simulations of homogeneous Poisson point pattern, with expected number of points $n = 200$ in $W \times T = [0, 10]^2 \times [0, 10]$, $\widehat{\rho^2} = 0.040$, $\epsilon = 0.735$ and $\delta = 0.248$.

Table 1 also shows the theoretical product density (ρ^2) under the Poisson case, together with the estimated average surface ($\widehat{\rho^{(2)}}_{\epsilon,\delta}(r, t)$), and the corresponding 5% and 95% sample quantile values for the product density ($Q_{5\%}(\widehat{\rho^{(2)}}_{\epsilon,\delta}(r, t))$ and $Q_{95\%}(\widehat{\rho^{(2)}}_{\epsilon,\delta}(r, t))$). Note that we have estimated ρ^2 by $\frac{n(n-1)}{(|W||T|)^2}$ which is an unbiased estimator in case of a homogeneous Poisson process (Stoyan & Stoyan 1994). Comparing the results in the fourth and eight columns, clearly the bias is negligible and $\widehat{\rho^{(2)}}_{\epsilon,\delta}(r, t)$ converges to ρ^2. In terms of variances, we present the approximate theoretical standard deviation surface ($\sigma(\widehat{\rho^{(2)}}_{\epsilon,\delta})$) together with the Monte Carlo mean estimate of the standard deviation surface ($\widehat{\sigma}(\widehat{\rho^{(2)}}_{\epsilon,\delta})$) obtained by simulation. Table 1 shows the results for only five selected cells (spatial and temporal lags (r, t)) over the fine grid of spatial and temporal distances to save space.

For illustrative purposes, the estimated product density function over the whole grid is depicted in Figure 1, for a homogeneous Poisson point pattern with intensity 0.2 in $W \times T$, and with $\epsilon = 0.735$ and $\delta = 0.248$. Figure 1(a) shows the average estimate of $\widehat{\rho^{(2)}}_{\epsilon,\delta}(r, t)$ under 100 repetitions of the selected scenario. Figure 1(a)

also presents the constant surface $\widehat{\rho^2}$ (which is equal to 0.040) for a homogeneous Poisson point pattern. Clearly $\widehat{\rho^{(2)}}_{\epsilon,\delta}(r,t)$ is an approximate unbiased estimator of $\rho^{(2)}(r,t)$.

Figure 1(b) shows the corresponding average estimate of the standard deviation surface under the same 100 repetitions. Figure 1(c) depicts the theoretical standard deviation surface coming from expression (6). Figure 2(a) shows the confidence surfaces for homogeneous Poisson point patterns based on the estimated product density and two standard deviations calculated using the expression of the variance in (6) together with a constant surface with value $\widehat{\rho^2} = 0.040$ and the average of the estimated product densities. We have obtained very similar results with intensities equal to 0.1 and 0.3, in simulations not shown here.

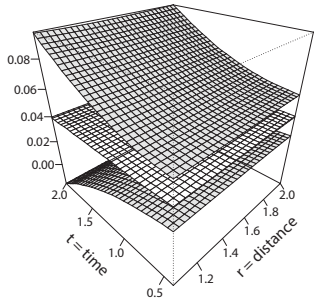

(a) Mean, homogeneous Poisson case (white), 0.98% confidence surfaces (lightgray) and theoretical product density (grey).

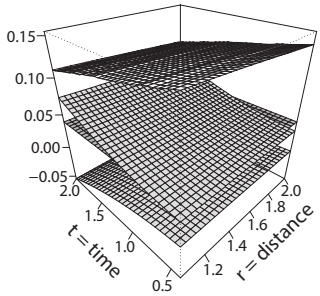

(b) Mean, inhomogeneous Poisson case (white), 0.98% confidence surfaces (lightgray) and theoretical product density (grey).

FIGURE 2: Mean estimate of the product density function in the inhomogeneous case with the very same region and expected number of points, $\epsilon = 0.99$ and $\delta = 0.38$.

Finally, Figure 2(b) shows the confidence surfaces for homogeneous Poisson point patterns with expected number of points $n = 200$ in $W \times T = [0,10]^2 \times [0,10]$ together with the average of estimated product densities coming from 100 inhomogeneous Poisson point patterns with intensity function given by

$$\rho(x,y,t) = \frac{ne^{20}}{10(e^{10}-1)^2} e^{-y-t}, \text{ with } (x,y,t) \in [0,10]^2 \times [0,10].$$

We note that the average surface for the inhomogeneous Poisson point pattern falls outside the confidence surfaces constructed under homogeneity.

6. Data Application: Invasive Meningococcal Disease

In this section, as a practical example, we illustrate how our product density estimator applies to Invasive Meningococcal Disease (IMD) data. IMD is a bacterial infection caused by bacterium Neisseria meningitidis. The data were previously analysed by Meyer et al. (2012) considering a mechanistic model with a conditional intensity function which is a superposition of additive and multiplicative components in space and time. The IMD data analysed in this section are taken from the R package surveillance (Höhle 2007).

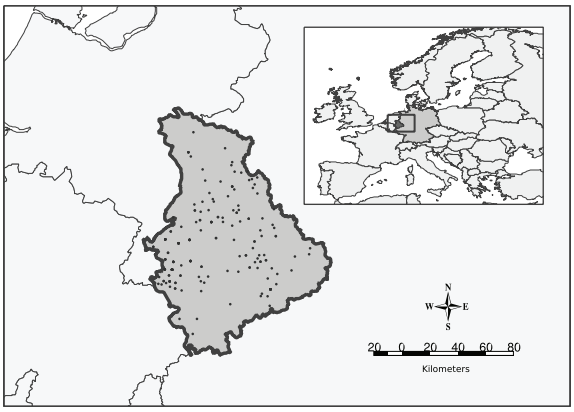

FIGURE 3: Subregion of Rhineland Regional Council (Germany).

The IMD data for the whole region of Germany shows a clear clustering behaviour (see Meyer et al. 2012), even without the help of any statistical tool. Therefore, we restrict our analysis to the subregion of Rhineland Regional Council (Germany) between 2003 and 2007 (see Figure 3), where the point pattern apparently does not show any clustering structure in space. The second-order analysis starts by applying a mechanism for visual assessment whether our point pattern is compatible with a spatio-temporal homogeneous Poisson pattern. If this hypothesis is rejected, the process can be modelled as a regular or as a cluster process. The area of this region is 9427.59 km^2 with a perimeter of 379.89 km. The IMD dataset consists of the spatio-temporal reports of 107 cases of IMD caused by two specific meningococcal finetypes, in which the times are given by 1491 days over the 5-years period, so the temporal region is defined as $T = [500.51, 1992.18]$. Figure 4(a) and Figure 4(b) show the estimated spatial and temporal intensities, respectively. In the purely spatial case, the pattern in Figure 4(a) does not exhibit any apparent clustering; for the time case, Figure 4(b) shows a nearly constant intensity indicating that temporal point pattern may be homogeneous.

Figure 5 shows the surface of the estimated second-order product density using $\epsilon = 7.72$ km and $\delta = 45$ days. We see large values for small spatial and temporal distances, which is a typical behaviour when spatio-temporal aggregation is present. However, the spatial aggregation decreases with increasing spatial

distances, while the temporal aggregation increases throughout the temporal distances. The clustering-type result is expected after visual inspection of Figure 5(a), and goes in the line found by Meyer et al. (2012).

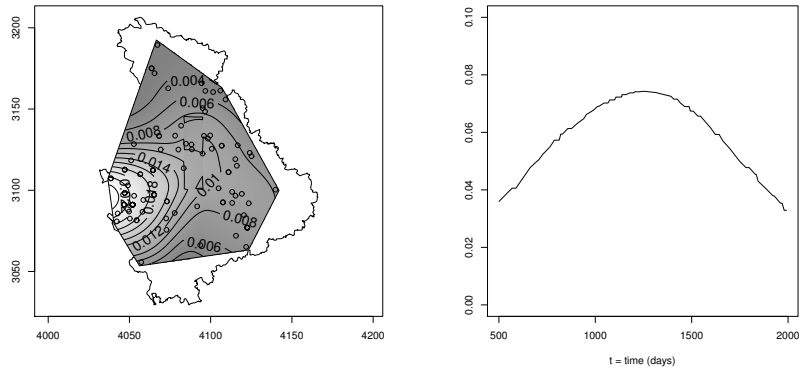

(a) Estimated spatial intensity. (b) Estimated temporal intensity.

FIGURE 4: Region of study, and estimated spatial and temporal intensities for the IMD dataset.

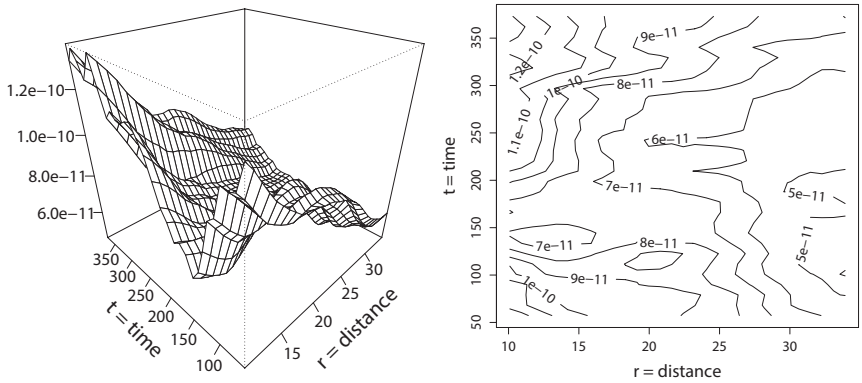

(a) Empirical surface. (b) Empirical contour.

FIGURE 5: Two estimation formats of the product density for IMD dataset with $\epsilon = 7.72$ km, and $\delta = 45$ days.

To emphasise this clustering behaviour, we also show in Figure 6 the empirical product density for the data together with simulated pointwise 95% envelope surfaces obtained from 39 simulations of spatio-temporal Poisson processes. Figure 6(a) considers homogeneous Poisson point patterns and we note that the surface of the empirical product density for the data does not have the constant shape that characterises a completely random point process. In addition, for small spatial distances $\widehat{\rho^{(2)}}_{\epsilon,\delta}(r,t)$ exceeds the upper envelope indicating clustering. Figure 6(b) considers inhomogeneous spatio-temporal Poisson processes with an

intensity built as the product of the spatial and temporal intensities for the IMD data; this plot shows a clear clustering behaviour as well.

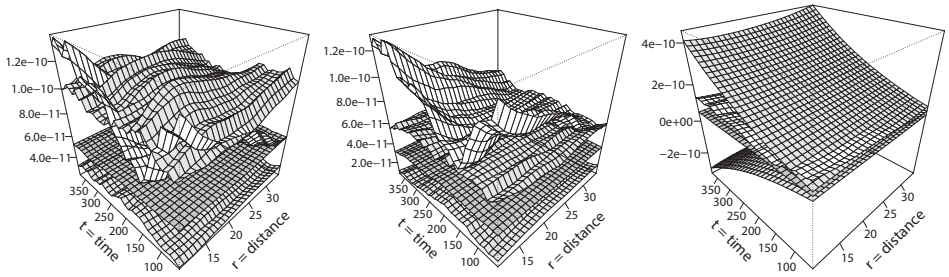

(a) Homogeneous (b) Inhomogeneous (c) Theoretical

FIGURE 6: Estimated product density function for the IMD data (white surface) together with simulated pointwise 95% envelope surfaces obtained from 39 simulations of: (a) homogeneous spatio-temporal Poisson point patterns; (b) inhomogeneous spatio-temporal Poisson point patterns with the estimated intensity function of IMD data (grey surfaces); (c) homogeneous Poisson point patterns using theoretical expressions (grey surfaces).

Note that in Figure 6(c) we construct the confidence surface under homogeneous Poisson point patterns based on the estimated $\widehat{\rho^{(2)}}_{\epsilon,\delta}(r,t) \pm 2 \times$ standard deviations calculated using the approximation of the variance in (6) for the empirical product density for the IMD data. Again, the empirical second-order product density exceeds the upper confidence surface. These three figures reveal that IMD has a contagious behaviour in their immediate spatio-temporal neighborhoods.

7. Discussion

The spatio-temporal product density describes second-order characteristics of point processes. It is useful to analyse the spatio-temporal structure of the underlying point process, and provides a natural starting point for the analysis of spatio-temporal point process data. It can be considered an exploratory tool, for check spatio-temporal inhomogeneity, clustering or interaction.

We have proposed a non-parametric edge-corrected kernel estimator of the product density under SOIRS hypothesis. The mean and variance of the estimator are obtained, and approximated closed form expressions are derived under the Poisson case. The pair correlation and K-functions are severely affected by the spatial and temporal intensity estimates as shown in Gabriel (2014). This is one of the reasons we propose in this paper using the product density. We indeed postulate the use of the second-order product density as it provides the same information, but with the added value that there is no need to estimate the spatio-temporal intensity. The main idea is to compare the fluctuation of the empirical

surface with the corresponding envelope and confidence surfaces, as a means to check for randomness and/or clustering, and also for model checking. The panels of Figure 6 show that confidence surfaces fluctuate only slightly more than the envelope surfaces. Therefore from the point of view of the computational cost, one can use the confidence surfaces instead of running 99 simulations to obtain envelope surfaces.

We have provided sufficiently statistical grounds in favour of using this second-order tool in the practical analysis of spatio-temporal point patterns. However, in our developments, we assumed that the point pattern is SOIRS. The statistical properties of the spatio-temporal product density under general non-stationarity conditions or anisotropic structures remain an open problem.

Acknowledgements

Research of J. Mateu were supported by the Spanish Ministry of Science and Education through the project MTM2016-78917-R.

[Received: January 2020 — Accepted: September 2020]

References

Adelfio, G. & Schoenberg, F. P. (2009), 'Point process diagnostics based on weighted second-order statistics and their asymptotic properties', *Annals of the Institute of Statistical Mathematics* **61**(4), 929.

Adelfio, G., Siino, M., Mateu, J. & Rodríguez-Cortés, F. J. (2020), 'Some properties of local weighted second-order statistics for spatio-temporal point processes', *Stochastic Environmental Research and Risk Assessment* **34**(1), 149–168.

Baddeley, A., Møller, J. & Waagepetersen, R. (2000), 'Non- and semi-parametric estimation of interaction in inhomogeneous point patterns', *Statistica Neerlandica* **54**, 329–350.

Berman, M. & Diggle, P. (1989), 'Estimating weighted integrals of the second-order intensity of a spatial point process', *Journal of the Royal Statistical Society: Series B (Methodological)* **51**(1), 81–92.

Chiu, S. N., Stoyan, D., Kendall, W. S. & Mecke, J. (2013), *Stochastic Geometry and Its Applications*, third edn, John Wiley and Sons.

Cox, D. R. & Isham, V. (1980), *Point Processes*, Chapman and Hall, London.

Cressie, N. & Collins, L. B. (2001a), 'Analysis of spatial point patterns using bundles of product density lisa functions', *Journal of Agricultural, Biological, and Environmental Statistics* **6**, 118–135.

Daley, D. J. & Vere-Jones, D. (2003), *An Introduction to the Theory of Point Processes. Volume I: Elementary Theory and Methods*, second edn, Springer-Verlag, New York.

Deng, H. & Wickham, H. (2011), Density estimation in R. Electronic publication.

Diggle, P. J. (2013), *Statistical Analysis of Spatial and Spatio-Temporal Point Patterns*, Chapman and Hall/CRC, Boca Raton.

Fiksel, T. (1988), 'Edge-corrected density estimators for point processes', *Statistics* **19**, 67–75.

Gabriel, E. (2014), 'Estimating second-order characteristics of inhomogeneous spatio-temporal point processes', *Methodology and Computing in Applied Probability* **16**(2), 411–431.

Gabriel, E. & Diggle, P. J. (2009), 'Second-order analysis of inhomogeneous spatio-temporal point process data', *Statistica Neerlandica* **63**, 43–51.

Gabriel, E., Rowlingson, B. & Diggle, P. J. (2013), 'stpp: An r package for plotting, simulating and analyzing spatio-temporal point patterns', *Journal of Statistical Software* **53**(2), 1–29.

Gabriel, E., Wilson, D. J., Leatherbarrow, A. J. H., Cheesbrough, J., Gee, S., Bolton, E., Fox, A., Fearnhead, P., Hart, C. A. & Diggle, P. J. (2010), 'Spatio-temporal epidemiology of campylobacter jejuni enteritis, in an area of Northwest England, 2000-2002', *Epidemiology and Infection* **138**(10), 1384–1390.

González, J. A., Hahn, U. & Mateu, J. (2020), 'Analysis of tornado reports through replicated spatiotemporal point patterns', *Journal of the Royal Statistical Society: Series C (Applied Statistics)* **69**(1), 3–23.

González, J. A., Rodríguez-Cortés, F. J., Cronie, O. & Mateu, J. (2016), 'Spatio-temporal point process statistics: A review', *Spatial Statistics* **18**, 505–544.

Guan, Y. (2007*a*), 'A composite likelihood cross-validation approach in selecting bandwidth for the estimation of the pair correlation function', *Scandinavian Journal of Statistics* **34**, 336–346.

Guan, Y. (2007*b*), 'A least-squares cross-validation bandwidth selection approach in pair correlation function estimations', *Statistics and Probability Letters* **77**, 1722–1729.

Guan, Y. (2009), 'On nonparametric variance estimation for second-order statistics of inhomogeneous spatial point processes with a known parametric intensity form', *Journal of the American Statistical Association* **104**, 1482–1491.

Hall, P. & Heyde, C. C. (2014), *Martingale limit theory and its application*, Academic press.

Höhle, M. (2007), 'surveillance: An R package for the monitoring of infectious diseases', *Computational Statistics* **22**(4), 571–582.

Illian, J., Penttinen, A., Stoyan, H. & Stoyan, D. (2008), *Statistical Analysis and Modelling of Spatial Point Patterns*, John Wiley and Sons, Chichester.

Meyer, S., Elias, J. & M. Höhle, M. (2012), 'A space-time conditional intensity model for invasive meningococcal disease occurrence', *Biometrics* **68(2)**, 607–616.

Møller, J. & Ghorbani, M. (2012), 'Aspects of second-order analysis of structured inhomogeneous spatio-temporal point processes', *Statistica Neerlandica* **66**(4), 472–491.

Møller, J. & Ghorbani, M. (2015), 'Functional summary statistics for the Johnson-Mehl model', *Journal of Statistical Computation and Simulation* **85**, 899–916.

Møller, J. & Waagepetersen, R. P. (2004), *Statistical Inference and Simulation for Spatial Point Processes*, Chapman and Hall/CRC, Boca Raton.

Ohser, J. (1983), 'On estimators for the reduced second moment measure of point processes', *Mathematische Operationsforschung und Statistik, series Statistics* **14**, 63–71.

Ripley, B. D. (1988), *Statistical Inference for Spatial Processes*, Cambridge University Press, Cambridge.

Sheather, S. J. & Jones, M. C. (1991), 'A reliable data-based bandwidth selection method for kernel density estimation', *Journal of the Royal Statistical Society. Series B (Methodological)* **53**, 683–690.

Siino, M., Rodríguez-Cortés, F. J., Mateu, J. & Adelfio, G. (2018), 'Testing for local structure in spatiotemporal point pattern data', *Environmetrics* **29**, 1–19.

Stoyan, D., Bertram, U. & Wendrock, H. (1993), 'Estimation variances for estimators of product densities and pair correlation functions of planar point processes', *Annals of the Institute of Statistical Mathematics* **45**, 211–221.

Stoyan, D. & Stoyan, H. (1994), *Fractals, Random Shapes and Point Fields*, Wiley, Chichester.

Wand, M. & Jones, M. C. (1994), *Kernel smoothing*, Chapman and Hall, London.

Wand, M., Moler, C. & Ripley, B. (2019), KernSmooth: Functions for Kernel Smoothing Supporting Wand & Jones (1995). R package version 2.23-16.
URL: *https://CRAN.R-project.org/package=KernSmooth*